

**COORDINATED OXYGEN ISOTOPIC AND PETROLOGIC STUDIES OF CAIS RECORD VARYING COMPOSITION OF PROTOSOLAR GAS.** J. I. Simon<sup>1</sup>, J. E. P. Matzel<sup>2</sup>, S. B. Simon<sup>3</sup>, P. K. Weber<sup>2</sup>, L. Grossman<sup>3</sup>, D. K. Ross<sup>1,4</sup>, and I. D. Hutcheon<sup>2</sup>. <sup>1</sup>NASA Johnson Space Center, Houston, TX 77058, USA (Justin.I.Simon@NASA.gov), <sup>2</sup>Lawrence Livermore National Laboratory, Livermore, CA 94551, USA, <sup>3</sup>The University of Chicago, Chicago, IL 60637, USA, <sup>4</sup>JE-23 Jacobs/ESCG, P.O. Box 58477, Houston, TX 77058.

**Introduction:** Ca-, Al-rich inclusions (CAIs) record the O-isotope composition of Solar nebular gas from which they grew [1]. High spatial resolution O-isotope measurements afforded by ion microprobe analysis across the rims and margin of CAIs reveal systematic variations in  $\Delta^{17}\text{O}$  and suggest formation from a diversity of nebular environments [2-4]. This heterogeneity has been explained by isotopic mixing between the  $^{16}\text{O}$ -rich Solar reservoir [6] and a second  $^{16}\text{O}$ -poor reservoir (probably nebular gas) with a “planetary-like” isotopic composition [e.g., 1, 6-7], but the mechanism and location(s) where these events occur within the protoplanetary disk remain uncertain.

The orientation of large and systematic variations in  $\Delta^{17}\text{O}$  reported by [3] for a compact Type A CAI from the Efremovka reduced CV3 chondrite differs dramatically from reports by [4] of a similar CAI, A37 from the Allende oxidized CV3 chondrite. Both studies conclude that CAIs were exposed to distinct, nebular O-isotope reservoirs, implying the transfer of CAIs among different settings within the protoplanetary disk [4]. To test this hypothesis further and the extent of intra-CAI O-isotopic variation, a pristine compact Type A CAI, Ef-1 from Efremovka, and a Type B2 CAI, TS4 from Allende were studied. Our new results are equally intriguing because, collectively, O-isotopic zoning patterns in the CAIs indicate a progressive and cyclic record. The results imply that CAIs were commonly exposed to multiple environments of distinct gas during their formation. Numerical models help constrain conditions and duration of these events.

**Samples:** Ef-1 is an  $\sim 3 \times 3.5$  mm convoluted compact Type A CAI composed mainly of melilite ( $\text{Åk}_{5-20}$ ) and 20-70  $\mu\text{m}$ -sized spinel locally enclosed by fassaite. It is surrounded by a  $\sim 15$  to 40  $\mu\text{m}$  thick Wark-Lovering (WL) rim composed from its interior outwards of spinel and pyroxene. TS4 is an  $\sim 5 \times 8$  mm irregularly shaped Type B2 CAI composed mainly of melilite ( $\text{Åk}_{35-50}$ ), fassaite, anorthite, and 5-70  $\mu\text{m}$ -sized spinel found throughout and as palisades. The fassaite and anorthite are found towards the interior and enclose high concentrations of spinel. TS4 is surrounded by a  $\sim 30$  to 50  $\mu\text{m}$  thick WL rim composed from its interior outwards of spinel, Ti-bearing pyroxene, Al-rich pyroxene, and an outermost band of forsterite. Secondary minerals include patchy sodalite at the edge of the CAI and discrete inclusions in the interior ([5], this meeting). A37 is described in [4].

**Methods:** We used the NanoSIMS at LLNL to perform O-isotopic measurements following the method developed by [4]. We evaluated instrumental mass fractionation (IMF) and reproducibility by analyses of terrestrial spinel, anorthite, grossular, and forsterite standards. O-isotope compositions are reported in terms of  $\delta^{17}\text{O}$  and  $\delta^{18}\text{O}$ . These values reflect the per mil difference from the reference ratios of standard mean ocean water (SMOW) such that  $\delta^i\text{O} = 10^3((^i\text{O}/^{16}\text{O})/(^i\text{O}/^{16}\text{O})_{\text{SMOW}} - 1)$  where  $i$  is either 17 or 18. Based on the range of standard analyses, the external precision was  $< 4.0\text{‰}$  (sd) for both ratios.  $\Delta^{17}\text{O}$ , defined as  $\Delta^{17}\text{O} = \delta^{17}\text{O} - 0.52\delta^{18}\text{O}$ , represents the departure from the terrestrial mass fractionation (TMF) line that defines the terrestrial oxygen reservoir. Our precision on  $\Delta^{17}\text{O}$  ranged from 1.9 $\text{‰}$  (sd) for olivine to 3.5 $\text{‰}$  (sd) for garnet and the difference in  $\Delta^{17}\text{O}$  among the terrestrial minerals was  $< 2.5\text{‰}$  (sd), about equal to, or less than our typical uncertainty ( $\sim 3.0\text{‰}$ ). Mineral compositions, x-ray, and backscattered electron maps were obtained at NASA-JSC, the University of Chicago, and LLNL to guide ion microprobe traverses and to verify the mineralogy of the analysis spots.

**Models:** Numerical solutions based on diffusional transport in a sphere were calculated to model the zoning profiles of the interiors of each CAI (Fig. 1A-C). Models assumed diffusive oxygen isotope exchange between CAIs and surrounding gas. Melilite data were primarily used to constrain the models. Models assumed continuity among melilite grains (i.e., volume diffusion throughout the CAIs). The O-isotopic compositions of spinel and pyroxene were used to infer initial gas compositions (in particular that in A37 that matches the initial Solar composition of [6]).

**Results:** O-isotope data for each inclusion come from  $\sim 2$   $\mu\text{m}$  spot analyses along traverses spanning across their WL rims and coarse-grained interiors (Fig. 1). Like A37, data from both Ef-1 and TS4 exhibit heterogeneous  $^{16}\text{O}$  abundances ( $> 20\text{‰}$ ). Yet, compared to A37, the interior melilites in Ef-1 and TS4 are more homogeneous and  $^{16}\text{O}$ -poor. Exceptions include systematic  $\Delta^{17}\text{O}$  decreases ( $\sim 5\text{‰}$ ) at the outermost edge of Ef-1 and possibly within the interior of TS4. Spinel from interiors of all studied CAIs are  $^{16}\text{O}$ -rich ( $\Delta^{17}\text{O} \leq -20\text{‰}$ ). The O-isotopic composition of fassaite in TS4 is similar to spinel, and that of anorthite in TS4 is similar to its melilite. Sodalite in the margin of TS4 has planetary-like,  $^{16}\text{O}$ -poor compositions. WL rims on

Ef-1 and TS4 are thinner and more difficult to sample than on A37. Yet, a similar isotopic stratigraphy exists within the minerals found in rims of all three CAIs: (1) spinel is  $^{16}\text{O}$ -rich ( $\Delta^{17}\text{O} \leq -15\text{‰}$ ); (2) pyroxene becomes relatively  $^{16}\text{O}$ -poor towards the interior; and (3) olivine varies systematically outward from  $\Delta^{17}\text{O} \leq -20\text{‰}$  to  $0\text{‰}$  once in TS4 and possibly twice in A37).

Melilite compositions for each CAI were collected in order to interpret the origin(s) of the O-isotope zoning profiles. Electron microprobe analyses were conducted along similar traverses as the ion probe analyses. As compared to melilite reported for A37 [4] and in the work by [3], which becomes progressively gehlenitic towards the inclusion rims, the melilite contained in both Ef-1 and TS4 is more homogeneous. This suggests that while CAIs studied by [3-4] may have had complicated exchange histories, possibly including partial melts, the oxygen zoning profiles of Ef-1 and TS4 likely formed in the solid-state.

**Discussion:** The mineral textures and compositions of the studied CAIs indicate crystallization from a melt (e.g., [8-9]). The O-isotope zoning in the studied CAIs reveal a progressive trend in the extent of exchange and number of distinct gas compositions recorded by Ef-1 > TS4 > A37 that is decoupled from their mineralogical evidence of alteration. At issue, are the differences found between the O-isotope zoning profiles among the studied CAIs (Fig. 1A-C) and the manner (solid  $\pm$  partial melt) in which the oxygen was exchanged and gas compositions subsequently recorded. The O-isotopic compositions of spinel from the interiors of Ef-1 and TS4 are similar to the  $^{16}\text{O}$ -rich melilites in the interior of A37. The difference between the  $^{16}\text{O}$ -poor compositions ( $\Delta^{17}\text{O} \sim 0\text{‰}$ ) of melilites in the interiors of Ef-1 and TS4 and their spinel ( $\pm$  fassaite) ( $\Delta^{17}\text{O} \sim -20$  to  $-25\text{‰}$ ) likely reflects their differing amounts of O-isotopic exchange with  $^{16}\text{O}$ -poor nebular gas. The new data on spinel ( $\Delta^{17}\text{O} \approx -30\text{‰}$ ) from A37 imply that the relatively less  $^{16}\text{O}$ -rich interior spinel data from Ef-1 and TS4 and melilite of A37 may also reflect variable exchange with a  $^{16}\text{O}$ -poor gas.

Model curves for Ef-1 reflect two periods of solid-gas exchange (Fig. 1A). The first step presumably included extensive equilibration of melilite with a planetary-like gas and the second step is consistent with 'recycling' into a relatively  $^{16}\text{O}$ -rich gas over timescales of  $80 \pm 20$  years at 1600 K. If correct, this is the first direct evidence that some CAIs (excluding evidence in their rims, cf., [3, 4]) were returned to a protosolar-like nebular gas. The zoning profile of TS4 suggests extensive exchange with a planetary-like gas (Fig. 1B). Given the "new" initial  $\Delta^{17}\text{O}$  ( $\approx -30\text{‰}$ ) value defined by spinel, a single step solution will not fit the zoning profile of A37 (e.g., note curvature of blue

curve in Fig. 1C). The data must then record an earlier sub-liquidus equilibration event, followed by a second step of solid-state diffusive exchange (e.g.,  $500 \pm 100$  years at 1600 K, [4]). Along with the additional WL rim data, the interior data strongly support the idea that CAIs were transported back and forth between two distinct nebular gases (and possibly a third with  $\Delta^{17}\text{O} \approx -20\text{‰}$ ) multiple times.

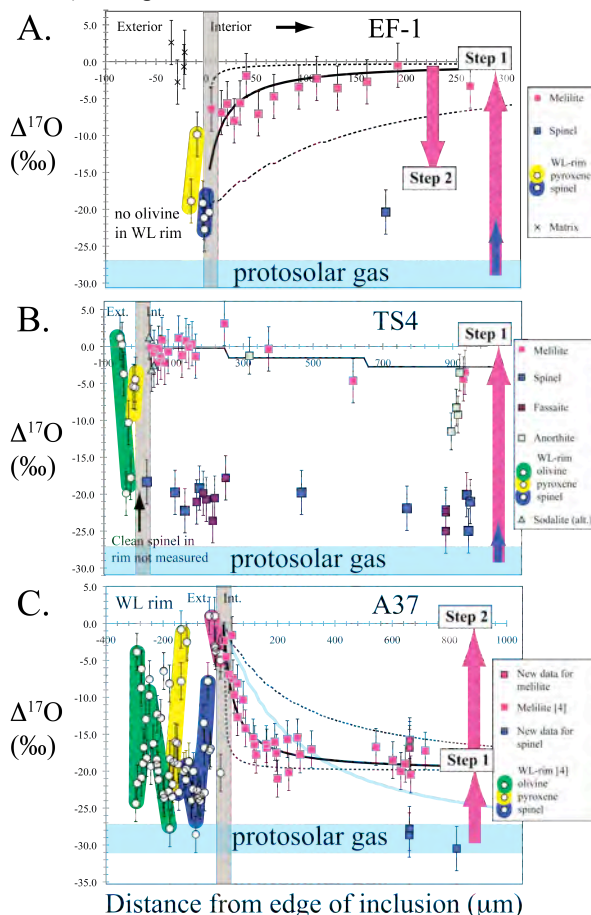


**Figure 1.** O-isotope zoning profiles across the WL rims and interiors of Ef-1, TS4, and A37, obtained by NanoSIMS. New data on spinel from A37 match the O-isotope composition of [6] and likely represent the primordial protosolar gas composition. Vertical arrows show the steps and varying magnitudes of mineral-gas exchange in the studied CAIs. Representative numerical solutions for diffusive O-isotope exchange to fit the melilite data are shown. Model fits to the distinct zoning profiles of Ef-1 and A37 require two steps (see text).

**References:** [1] Clayton, R.N. et al. (1977), *EPSL* 34, 209-224. [2] Itoh S. and H. Yurimoto (2003) *Nature*, 423, 728-731. [3] Aleon, J. et al. (2007) *EPSL*, 263, 114-127. [4] Simon, J.I. et al. (2011) *Science*, 331, 1175-1178. [5] Ross et al., this meeting. [6] McKeegan, K.D. et al. (2011), *Science* 332, 1528-1532. [7] Ryerson, F.J. and K.D. McKeegan (1994) *GCA* 58, 3713-3734. [8] MacPherson, G.J., and L. Grossman (1981) *EPSL* 52, 16-24. [9] Simon, S.B. et al. (1999) *GCA* 63, 1233-1248.